

# THE STUDY OF BEAM-BEAM EFFECTS ON BINP ELECTRON-POSITRON COLLIDERS

V. Borin<sup>1</sup>, V. Dorokhov, G. Karpov, O. Meshkov<sup>1</sup>, D. Shatilov, D. Shwartz<sup>1</sup>, M. Timoshenko  
 The Budker Institute of Nuclear Physics, Novosibirsk, Russia  
<sup>1</sup> also at Novosibirsk State University, Novosibirsk, Russia

## Abstract

The beam-beam effects depending on the beams current and energy were studied at electron-positron collider VEPP-2000 by the set of different diagnostics: the streak camera, optical dissector, BPM. The beam transverse profiles as well as longitudinal motion were acquired from the moment of a first collision of the beams in the interaction point up to the establishment of an equilibrium state. The spectra of the beams oscillation during this process were studied. The obtained results are discussed.

## INTRODUCTION

VEPP-2000 is a small 24 m perimeter single-ring collider operating in one-by-one bunch regime in the energy range below 1 GeV per beam [1]. Its layout is presented in Fig. 1. Collider itself hosts two particle detectors [2, 3], Spherical Neutral Detector (SND) and Cryogenic Magnetic Detector (CMD-3), placed into dispersion-free low-beta straights. The final focusing (FF) is realized using superconducting 13 T solenoids. VEPP-2000 exploits the round beam concept [4]. This approach, in addition to the straightforward geometrical gain factor in luminosity should yield the beam-beam limit enhancement.

## BEAM-BEAM INTERACTION

VEPP-2000 has no beam vertical separation, thus the beams collide in two interaction points right after injection. It is of special importance during injection phase because of the strong beam-beam interaction influence on the beam dynamics.

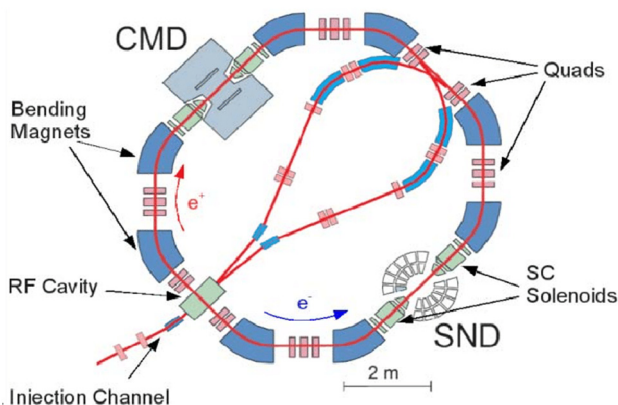


Figure 1: VEPP-2000 layout.

The recently achieved luminosity of VEPP-2000 in comparison to 2010–2013 performance is shown in Fig. 2. In the middle energy range the achieved luminosity is well

above all expectations. At the same time at top energy luminosity is lower than design value in a factor of two. The absolute record for today VEPP-2000 peak luminosity of  $5 \times 10^{31} \text{ cm}^{-2} \text{ s}^{-1}$  was achieved at the energy of 550 MeV per beam. The next Fig. 2 presents the integrated by CMD-3 detector luminosity over all operating years since VEPP-2000 commissioning. One should beware of direct comparison of different runs integrals due to luminosity dependence on energy. 2012/13 and 2017/18 runs were spent for data taking below 500 MeV while the others were dedicated to higher energies

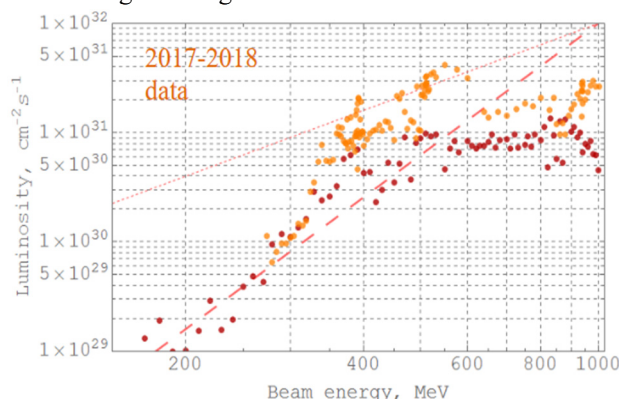


Figure 2: CMD-3 recorded in 2010–2013 (crimson) and in 2017–2018 (orange) luminosity averaged over 10% of best runs. Pink lines show scaling laws with fixed (dashed line) and variable (dotted line)  $\beta^*$ .

We have decided to develop the diagnostics and to conduct the experiments aimed on the study of beam-beam effects which, presumably, restrict the luminosity of the collider. The first run was made with non-complete set of the diagnostics tools but the obtained results allowed us to separate some symptoms of beam-beam interaction revealing in longitudinal and transverse beams dynamics.

## STREAK-CAMERA MEASUREMENTS

In order to observe longitudinal beam motion in turn by turn mode the “PS-1/S1” streak camera [5] was implemented into electron optical diagnostics of the VEPP-2000. The camera has a temporal resolution about 3 ps. Moreover, we have observed not only the longitudinal beam profile but also received data about vertical beam profile and dynamics.

Start of steak camera image acquisition was coordinated with the moment of the beam injection and can be delayed turn by turn. Each new image is the new injected beam. Thus we had to precisely control currents of stored and in-

jected beam in order to reproduce measurement's conditions. The threshold currents restricted by beam-beam effects were empirically determined during routine collider runs. All measurements were conducted at these high currents in order to create strong beam-beam effect accompanied by the lost of injected beam.

### Injection of $e^-$ to Circulating $e^+$

If we inject about 40 mA of electrons into ring with 65 mA circulating positrons than after several turns we see that the head of injected electron beam starts to split into non equal parts (Fig. 3). At 80 turns after the injection the lower part of splitted beam is almost disappears.

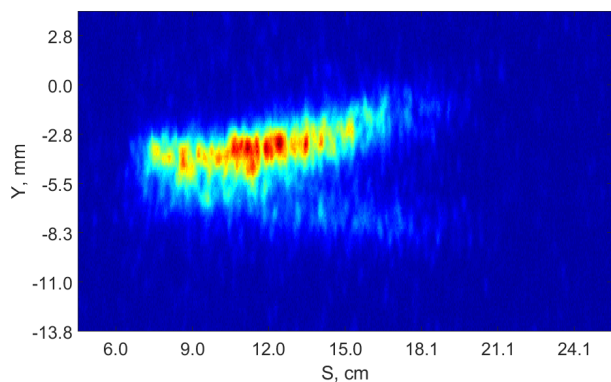


Figure 3: Split of electron beam head in 40 turns after the injection to circulating positron beam.  $I_e=30$  mA,  $I_p=66$  mA.

This effect depends on the relation between positron and injected electron beam currents. Our aim for the nearest future is to observe this process in more details in time scales more than 80 turns after the injection.

### Injection of $e^+$ to Circulating $e^-$

When a positron beam is injected to an electron beam and positron beam is lost during this process we observe some deviations in electron beam dynamics. The example is shown in Fig. 4.

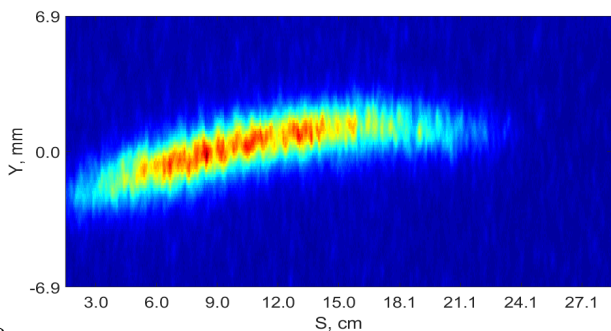


Figure 4: Deflection of electron beam in Y-S plane in 40 turns after the injection of positron beam.  $I_e=66$  mA,  $I_p=45$  mA.

It is seen that electron beam is deflected in Y-S plane respectively to its stable condition. On Y axis zero coordinate remarks stable beam position. In Fig. 5 position of the

beam center is shown with different injected and stored beam currents. One can notice that deflection depends on relation between beam currents.

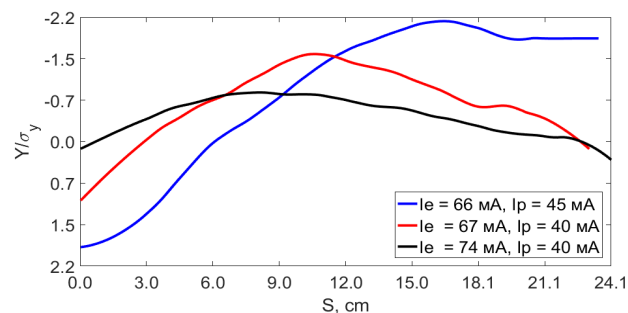


Figure 5: Deflection of electron beam in Y-S plane acquired at 40 turn after the injection of positron beam with different relation of the beam currents.

### Injection of $e^-$ to Circulating $e^-$

When an electron beam is injected into empty ring or to circulating electron beam there were no abnormal behaviour registered (Fig. 6).

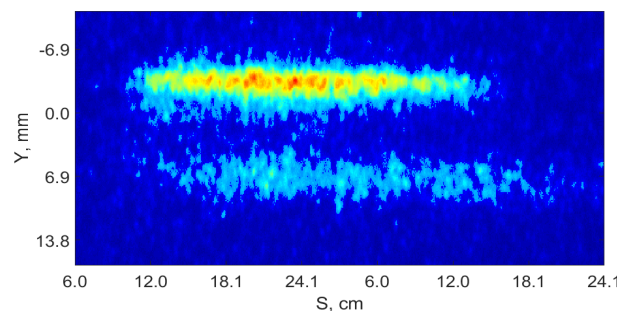


Figure 6: Injection of 12 mA of electrons (lower image) to 18 mA of circulating electrons (upper image). No profile distortions are seen.

## TRANSVERSE BEAM PROFILE MEASUREMENTS

In order to understand transverse beam dynamics during the injection we used 16-elements optical detector based on avalanche photodiode array [6]. The detector acquired a dynamics of radial profile of the beam during 2730 turns.

During the injection cycles we have observed the strong betatron oscillations of beam center and the beam size (Fig.7).

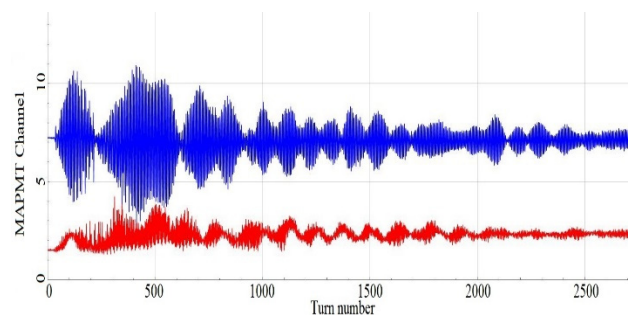


Figure 7: Positron beam injection into the ring with circulating electrons. Red line – beam size, blue line – position of beam center.

If we take Fourier transformation of these signals then we see that beam size oscillates with betatron frequency, while beam position oscillates on the second betatron tune harmonic (Fig. 8).

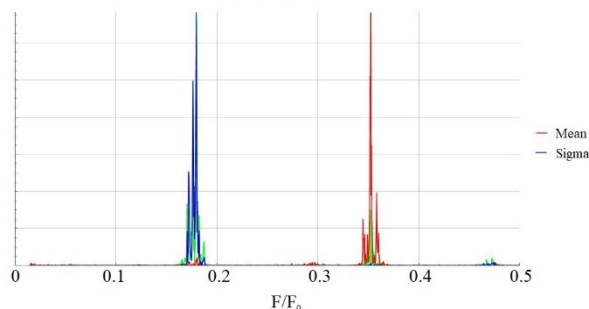


Figure 8: Fourier transformation of electron beam oscillations during the positron beam injection into the ring.

## OPTICAL DISSECTOR MEASUREMENTS

We have applied the optical dissector [7] in the mode of “phase slit” for turn by turn observation of longitudinal beam oscillations during injection. Dissector has recorded an amplitude on the slope of the longitudinal beam profile in a selected phase. Thus tuning the device with the slope of the stable beam we were able to record all kinds of beam longitudinal oscillations appearing after injection. In Fig. 9 spectrum of injected electron beam oscillations is shown.

One can clearly see up to 5<sup>th</sup> harmonics of synchrotron oscillations, but it almost impossible to detect synchrotron frequency in this spectrum.

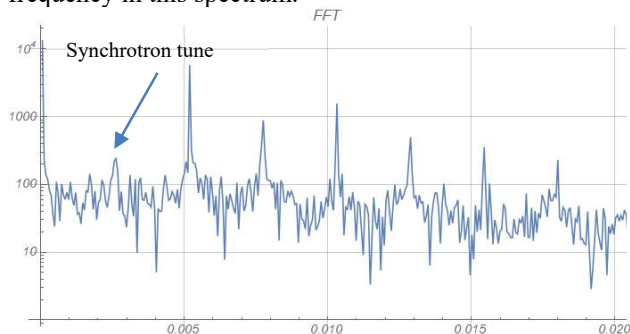


Figure 9: Fourier transformation of electron beam longitudinal oscillations during the positron beam injection into the ring.  $I_e=8$  mA,  $I_p=71$  mA.

But if we inject beam into an empty ring, where there is no beam-beam effects which we need to take into account in order to explain this complicated spectrum such as shown above, then we see simple synchrotron spectrum as shown in Fig. 10.

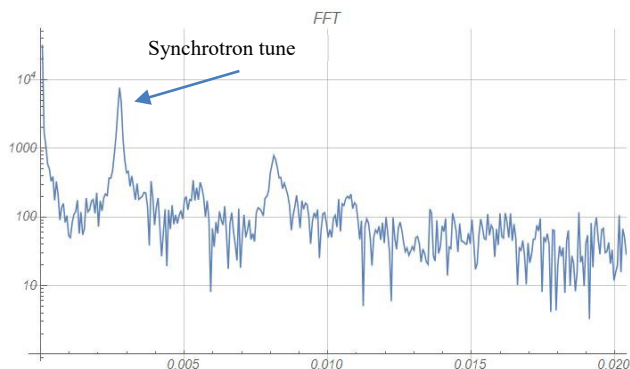


Figure 10: Fourier transformation of electron beam longitudinal oscillations during an injection into the empty ring,  $I_e=20$  mA.

## CONCLUSION

We have started studies of beam-beam effects and beam dynamics during the injection. First obtained data are presented. Our plans for the nearest future are to upgrade measurement system installing more detectors for acquisition of transverse profiles of both beams and to record the beam dynamics during longer temporal intervals. We want also to simulate a beam behaviour and compare it with experimental results. The final goal is to understand and overcome the reasons restricting a performance of VEPP-2000.

## REFERENCES

- [1] Yu. M. Shatunov *et al.*, "Project of a New Electron-Positron Collider VEPP-2000", in *Proc. EPAC'00*, Vienna, Austria (2000) pp. 439-441.
- [2] A.A. Korol *et al.*, "Recent Results from the SND Detector", *Phys. Part. Nucl.* 49 (2018) no.4, pp. 730-734.
- [3] R.R. Akhmetshin *et al.*, "Hadronic cross sections with the CMD-3 detector at the VEPP-2000", *Nucl. Part. Phys. Proc.*, vol. 294-296 (2018) pp. 170-176.
- [4] V.V. Danilov *et al.*, "The Concept of Round Colliding Beams", in *Proc. EPAC'96*, Sitges, Spain (1996) pp. 1149-1151.
- [5] S.G. Garanin *et al.*, "PS-1/S1 picosecond streak camera application for multichannel laser system diagnostics", *Quantum Electron.*, vol. 44 no. 5, p. 798, 2014.
- [6] O. Meshkov *et al.*, A new station for optical observation of electron beam parameters at electron storage ring SIBERIA-2. *Journal of Instrumentation* 12/2016; 11(12):P12015-P12015., DOI:10.1088/1748-0221/11/12/P12015
- [7] E.I. Zinin *et al.*, Direct temporal-resolution calibration of new-generation dissector. *Journal of Instrumentation* 03/2016; 11(03):T03001-T03001., DOI:10.1088/1748-0221/11/03/T03001